11 Factors Governing the Structure of Volcanic Jets

SUSAN WERNER KIEFFER
U.S. Geological Survey

ABSTRACT

Observable characteristics of volcanic jets, such as temperature, shape, and velocity, depend in a complex way on the subsurface features of the volcanic systems from which the jets emanate. The variety of sizes and shapes of jets associated with violent eruptions reflects differences primarily in the geometric shapes of the near-surface parts of the volcanic systems and, secondly, differences in thermodynamic properties and rheology of the erupting fluids. In this paper, differences in shape between plinian eruption columns and lateral blast flows on Earth and between umbrella-shaped and diffuse plumes on Jupiter's moon, Io, are discussed in terms of a generalized model for thermodynamic properties and geometry of a volcanic system. On Earth, decompression of the volcanic fluid to ambient pressure of 1 bar typically occurs within only a few tens of meters from the bottom of a crater. In contrast, ambient subsolar surface pressure on Io is about 10^{-12} bar (perhaps as high as 10^{-7} bar in the vicinity of an erupting volcano), and the pressure in a jet on Io will decay from the sonic conduit value to ambient within the crater only if the crater is more than 1 km deep. Therefore, on either body, two classes of jets may result from different crater depths: (1) "pressure-balanced" jets, if the jet pressure approximately equals ambient pressure as it emerges at the surface of the planet, or (2) "overpressured" (underexpanded) jets, if the jet pressure greatly exceeds atmospheric. The structure of pressure-balanced jets may vary from one planet to another, but on one planet the jets may tend to have rather similar structures from one volcano to another because they are equilibrated to atmospheric pressure. The structure of pressure-balanced jets is determined primarily by the initial thrust and, secondly, by external factors such as entrainment of air, winds, and mixture buoyancy. These factors also influence overpressured jets, but internal jet dynamics, including shock and expansion waves, also play a significant, sometimes dominant, role. Overpressured jets may show a much greater diversity in structure than pressure-balanced jets because the jet structure depends on the ratio of jet pressure to atmospheric pressure and typical volcanic eruption conditions allow a wide range of ratios. Plinian eruption columns are typical terrestrial pressure-balanced jets because they commonly emerge through craters and thus enter the atmosphere at atmospheric pressure. Plume 3 (Prometheus) on Io may be pressure matched to the Ionian atmosphere. The lateral blast of May 18, 1980 at Mount St. Helens was an overpressured jet, since it emerged directly at high pressure from the face of the mountain; it was able to expand toward atmospheric pressure only as it traveled tens of kilometers away from the mountain. On Io, plume 2 (Loki), which apparently emerges through a fissure, may have been overpressured when photographed during Voyager 1.

INTRODUCTION

The verb *to explode* is defined by *Webster's Third New International Dictionary* as "(1) to undergo rapid combustion with sudden release of energy in the form of heat that causes violent expansion of the gases formed and consequent production of great disruptive pressure and a loud noise, (2) to undergo an atomic nuclear reaction with similar but more violent results, and (3) to burst violently as a result of pressure from within." Although our understanding of the thermodynamic evolution of magma before and during an eruption has increased enormously over the last few decades (Graton, 1945; Verhoogen, 1946; Boyd, 1961; Sparks *et al.*, 1978; Self *et al.*, 1979; Wilson and Head, 1983), many misconceptions remain of processes occurring during explosive volcanism. This paper describes how jets from violently erupting volcanoes obtain their "explosive" velocities from the transformation of the initial enthalpy stored in magma into kinetic energy and how the transformation process depends on the interplay between the system geometry, fluid thermodynamic properties, reservoir initial conditions, and ambient atmospheric conditions. The concepts are applied to an interpretation of the structure of four jets of very different shapes: (1) the lateral blast that initiated the eruption on May 18, 1980, at Mount St. Helens; (2) the plinian plume that developed during the same eruption; (3) the umbrella-shaped plume of many volcanoes, such as Prometheus, on Jupiter's satellite, Io; and (4) the diffuse plume of Loki on Io. Further details are given in Kieffer (1981, 1982a, 1982b).

VOLCANIC JETS*

The fact that volcanic jets associated with violent eruptions come in a variety of sizes and shapes (see Figure 11.1) has important implications for understanding the relationships between jet structure, magma properties, and volcanic system geometries as well as for volcanic hazard modeling and comparative planetology. Two very different jet structures were evident during the course of the eruptions on May 18, 1980, at Mount St. Helens. The vertical jet that developed as the May 18 eruption sequence progressed (Figure 11.1a) is typical of jets from major plinian eruptions on Earth. The jet was a towering column of gas and pyroclastics and resembled a jet of water from a fire hydrant in that most of the flow was directed upward and was approximately parallel to the presumed vertical center line of the conduit from which it erupted. The columnar form occurred because material in the column maintained the vertical direction of motion imparted by accelerations in the volcanic system. Convective mixing of air into the eruption column caused the column to grow slowly wider with height, but not until the plume reached altitudes at which it became neutrally buoyant did interactions with major atmospheric layers cause it to deviate from the columnar form.

In contrast, the jet of the lateral blast that initiated the May 18 eruption was very different in shape. The shape of the lateral blast is reflected in the shape of the devastated area north of the volcano where the blast was sufficiently dense to remain near the ground; at a distance of about 25 km it became buoyant enough to lift from the land. Photographs of the inception of the blast show that initial particle motions were largely directed northward. However, over much of the region covered by the jet, the streamlines and the flow boundaries were *not* directed northward. In contrast to the way that the material in the plinian column maintained its initial direction of motion, the material in the lateral blast departed from the initial direction as soon as it left the face of the mountain. The flow initially spread out over a broad fan-shaped sector diverging around the mountain as far as southeast and southwest (see Figure 11.1b). The overall shape differences between the columnated vertical plume and the fanning lateral blast cannot be explained by differences in the orientation (vertical versus subhorizontal) of the jets alone, and the intriguing question of why the shapes of the two jets at Mount St. Helens were so different remains.

Observations by Voyager spacecraft show that jets also come in a variety of shapes on Io, the only other planet in the solar system where current volcanic activity exists (Strom *et al.*, 1979; Strom and Schneider, 1982; McEwen and Soderblom, 1983). The volcanoes on Io seem to have two types of behavior. One group of volcanoes (Pele, Surt, Aten Patera) have short-lived eruptions (days to weeks probably), eject plumes to heights of ~300 km, and deposit ejecta of sulfur in discrete rings at distances up to 1400 km from the vent. Surface temperatures near the source regions are in the range of 500 to 700 K. The other group of volcanoes (Prometheus, Volund, Amirani, Maui, Marduk, Masubi, and two plumes from Loki) are long lived (years), eject plumes to heights on the order of only 100 ± 40 km, and deposit white ejecta (SO_2?) in discrete rings of only 200 to 300 km diameter or in diffuse rings. They have surface temperatures near the source regions that are less than 400 K. McEwen and Soderblom (1983) suggested that these two differences in class represent sulfur- versus sulfur-dioxide-driven plumes. Deposits from Loki suggest that it varies between the two classes in behavior, but for the purposes of this discussion its behavior while it appeared to be in the second group during the Voyager 1 encounter is analyzed.

Of particular interest here is the fact that most of the plumes have beautiful umbrella shapes and deposit ejecta in discrete rings (e.g., Pele, Surt, Aten Patera, Maui, Prometheus) (see Figure 11.1c). However, Loki (plume 2, Figure 11.1d) and Volund, as observed by Voyager 1, have more diffuse plumes and more irregular deposits.

*The gas-particulate emissions from volcanoes have commonly been referred to as *plumes*, which, by strict definition, resemble a feather in shape, appearance, or lightness. In the more rigorous fluid mechanics context, a plume is buoyancy dominated. Thus, a volcanic plume is generally thought of as a rising buoyant column of gas with entrained pyroclastic fragments. However, the emissions from many violent eruptions are unfeatherlike in shape, appearance, or lightness, e.g., nuées ardentes, lateral blasts, and other such dense flows. The word *jet* is used in fluid mechanics to describe a general flow from an orifice and, more specifically, refers to a flow that is momentum dominated. In this paper, I use the word *jet* in a more general context than the word *plume*.

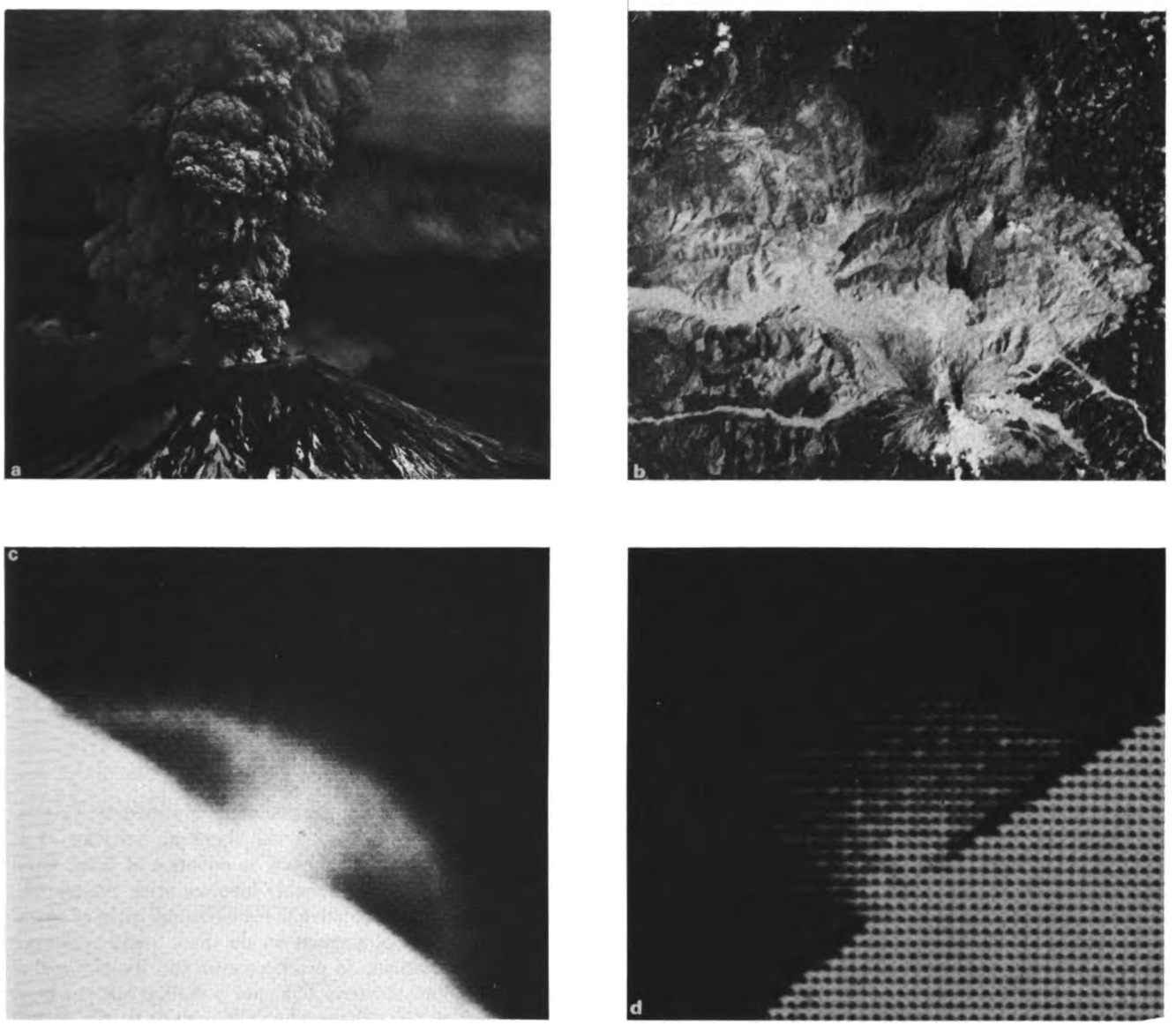

FIGURE 11.1 Eruption jets on Earth and on Io. (a) The plinian eruption column at Mount St. Helens, May 18, 1980. The crater from which the plume emerges is approximately 1 km in diameter. Photograph by Austin Post, U.S. Geological Survey. (b) Satellite photo of the area devastated by the lateral blast on May 18, 1980, at Mount St. Helens (EROS Data Center, Goddard Space Flight Center). The distance from the mountain to the farthest northwest and northeast boundaries of the devastated region is about 25 km. The devastated area is assumed to mimic the shape of the jet from the lateral blast over the area where the jet remained close to the ground. The jet actually extended beyond these boundaries but lifted from the ground when it expanded to ambient atmospheric density (Kieffer, 1982a). (c) Umbrella-shaped plume 3 from Prometheus on Io. The jet is about 70 km high (image by NASA). (d) Diffuse plume 2 from Loki on Io. The jet is 165 km high (image by NASA).

VOLCANIC SYSTEM GEOMETRY

The structure of volcanic jets cannot be isolated from the behavior of magmatic fluid in subsurface parts of a volcanic system. To analyze jet structure, the fluid composition, the mechanical behavior, and flow conservation laws through all parts of the volcanic system must be considered. To formalize these assumptions, I have divided a volcanic system into five regions that are separately susceptible to analysis of fluid dynamic and thermodynamic behavior: *supply region*, in which magma is generated; *reservoir*, in which it collects; *conduit* and *crater*, in which accelerations to high velocities can occur; and *jet or*

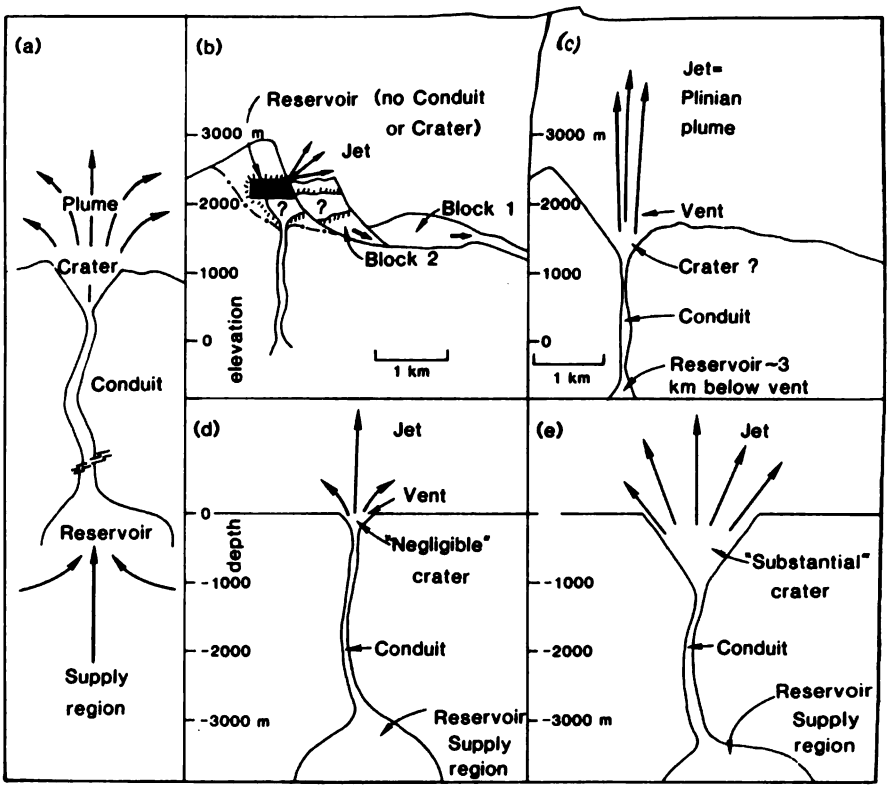

FIGURE 11.2 Schematic geometry of volcanic systems used for models discussed in text. (a) Sketch illustrating the concept of the five parts of a volcanic system discussed in the text. (b) Model for simple, direct discharge of reservoir into jet at Mount St. Helens for lateral blast. Blocks 1 and 2 represent the two major blocks involved in the landslide (after Moore and Albee, 1982). The stippled area surrounded by hachuring represents the combined magmatic-hydrothermal system assumed to have underlain the north slope of the mountain; configuration is unknown. The complex reservoir geometry that fed the blast is simplified by assuming that the material discharged from a tabular reservoir that was 1 km in east-west dimension, 0.25 km in vertical height, and 0.5 km in north-south depth. It is assumed that the flow of the dacite from the deep reservoir (as illustrated in sketch c) was not involved in the lateral blast. (c) Discharge of deep reservoir through conduit and, perhaps, the shallow surface crater into jet to form plinian eruption column at Mount St. Helens. (d) Discharge of reservoir through conduit with negligible surface crater on Io (called a *fissure system*). (e) Discharge of reservoir through conduit with substantial surface crater on Io (called a *crater system*).

plume, the visible ejecta above the planetary surface (see Figure 11.2a). The geometry of a volcanic system is unique to each volcano and, perhaps, even to each eruption at a given volcano.

Consider nominal system geometries for the four examples under discussion. The lateral blast at Mount St. Helens is modeled as the discharge of a simple, shallow, tabular reservoir exposed suddenly to atmospheric pressure by the landslide that initiated the eruption at 8:32 A.M. (Figure 11.2b). The tabular shape is compatible with observations that the discharge occurred over a surface area at least 1 km in lateral dimension and 0.25 km in height and that about 0.25×10^{15} g of material were ejected. However, it is a much oversimplified representation of a reservoir that was certainly complex in geometry and in temporal evolution. The plinian eruption at Mount St. Helens is modeled as the discharge of a deeper (~3 to 5 km) reservoir through a conduit, with perhaps a crater (Figure 11.2c). This model is consistent with seismic observations of the depth of emplacement of magma by May 18.

The Ionian eruptions are modeled as the discharge of shallow crustal reservoirs through cylindrical or tabular conduits several kilometers deep, similar to the plinian system assumed for Mount St. Helens. One system, which for convenience I call a fissure system, is assumed to have no substantial surface crater (Figure 11.2d). The other system, which I call a crater system, has a substantial surface crater (Figure 11.2e). (A substantial surface crater will be defined later in this paper.) I will demonstrate that the geometry of a volcanic system in the near-surface region has a larger influence on the structure of a volcanic jet than do plausible variations in thermodynamic properties of the magma and initial pressure conditions.

THERMODYNAMIC PROPERTIES OF MAGMATIC FLUIDS

In addition to simplifying the geometry of a volcanic system, it is also necessary to simplify the rheologic behavior of its magmatic fluid in order to obtain an equation of state. Even though magmatic ascent probably involves many nonequilibrium processes, representative thermodynamic paths of ascent on phase diagrams of magmas would show useful reference equilibrium conditions. In practice, even this limited goal of showing equilibrium thermodynamic paths has not yet been done for any magma. Thermodynamic analysis is still limited to highly idealized fluids by two constraints: (1) the properties of magmas are so complex that complete phase diagrams have not yet been formulated, and (2) the equations describing fluid flow can be solved only for the simplest equations of state and thus cannot accommodate the complexities that are necessary to describe magma flow, e.g., phase changes, gas-liquid-particle interactions, radiative heat transfer.

Magma rheology is conveniently simplified by recognition of three types of fluid behavior corresponding to decreasing depth in the volcanic system (Wilson *et al.*, 1980): (1) the *lower zone*, where volatiles are dissolved in the magma; (2) the *middle zone*, where the volatiles are exsolved within a liquid phase; and (3) the *upper zone*, where the volatiles are the dominant phase by volume and the magma is a gas with entrained liquid droplets and solid fragments. These three rheologic zones need not, of course, correspond to any idealized geometric zones in a volcano. For example, fragmentation (upper-zone behavior) may occur deep in a conduit, or even within a reservoir, in a

deep-seated kimberlite or caldera eruption, whereas liquid magma with little exsolved gas may appear in surface craters in Hawaiian eruptions. In this paper I discuss systems in which the rheology is gas dominated at the conduit level.

Much can be illustrated about the thermodynamics of upper-zone magmatic behavior by considering the phase diagrams of the volatiles that propel the ascent of magma, because most of the velocity during ascent is obtained after the magma has fragmented into a gas-pyroclast mixture (see Wilson *et al.*, 1980). Therefore, if hypothetical initial states for the volatile components of a magma can be specified from knowledge of pressure-temperature relations in volcanic regions (geotherms on the Earth, iotherms on Io), the thermodynamic history of the volatiles can be outlined and the thermodynamic history of the magma approximated. The pressure-temperature phase diagrams of H_2O, CO_2, SO_2, and S are shown in Figure 11.3 with superposed geotherms and iotherms. These diagrams provide the initial pressures and temperatures for solution of the fluid flow equations. The thermodynamic history of the fluids during ascent and eruption, however, is more easily analyzed on temperature-entropy (T-S) phase diagrams, shown in Figure 11.4, because many eruptions are quasi-isentropic and analysis of the fluid flow is often restricted by the assumption of isentropic processes. Even if the expansion of the erupting volatile

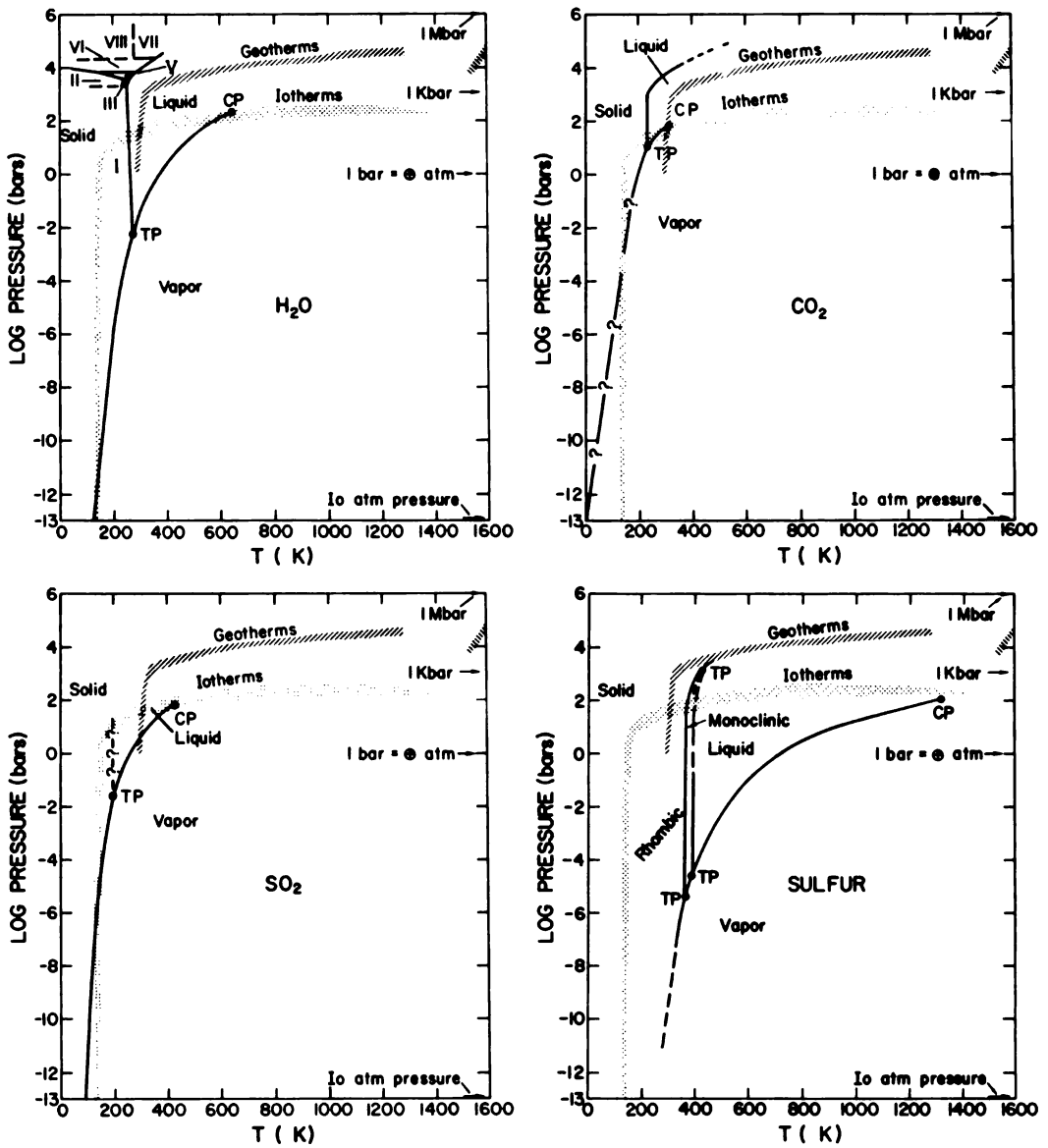

FIGURE 11.3 Geotherms and iotherms superposed on phase diagrams of H_2O, CO_2, SO_2, and S. This figure reproduced from Kieffer (1982b, with permission of the the University of Arizona Press), where data sources for the phase diagrams and phase diagrams can be found in the caption to Figure 18.3.

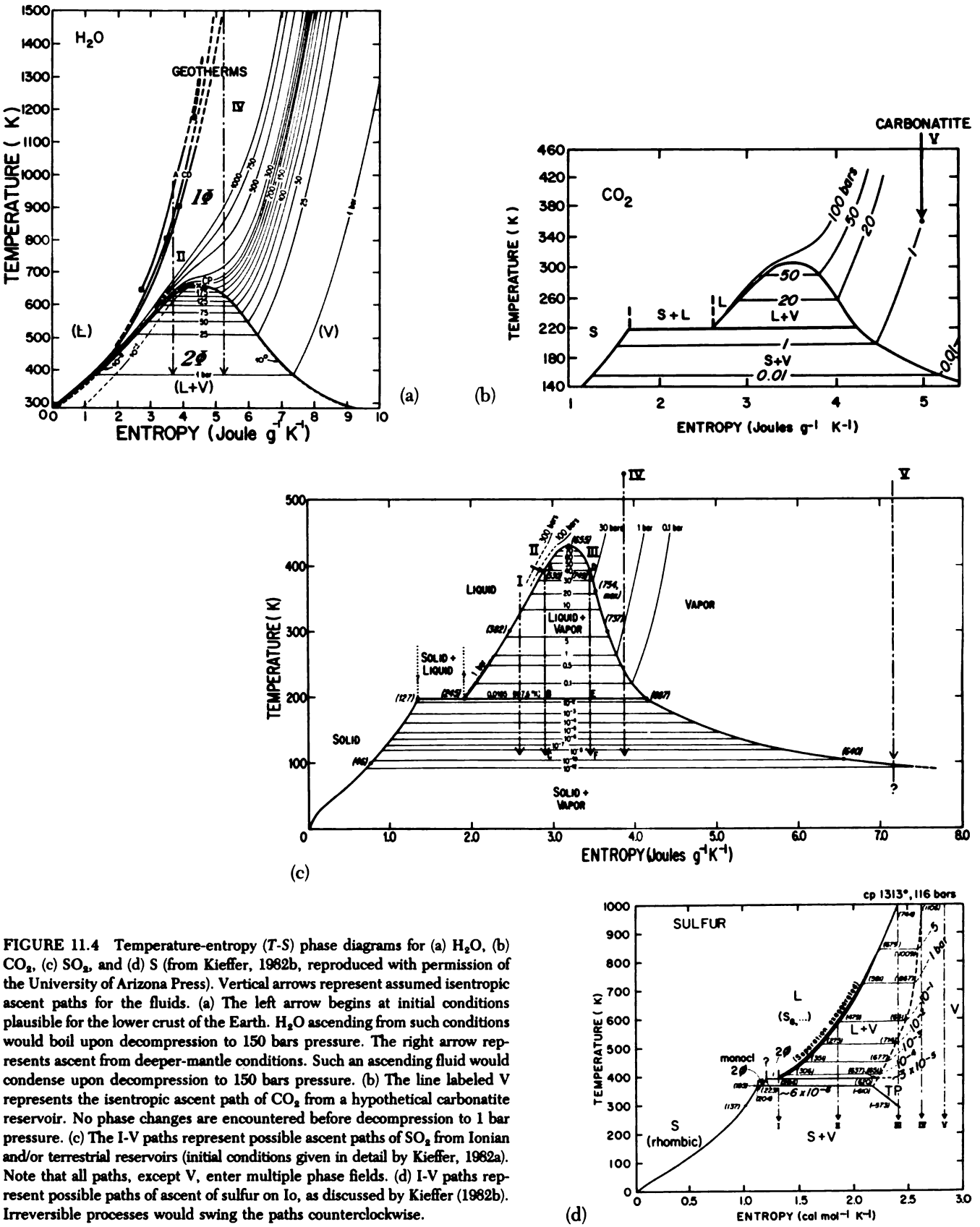

FIGURE 11.4 Temperature-entropy (T-S) phase diagrams for (a) H_2O, (b) CO_2, (c) SO_2, and (d) S (from Kieffer, 1982b, reproduced with permission of the University of Arizona Press). Vertical arrows represent assumed isentropic ascent paths for the fluids. (a) The left arrow begins at initial conditions plausible for the lower crust of the Earth. H_2O ascending from such conditions would boil upon decompression to 150 bars pressure. The right arrow represents ascent from deeper-mantle conditions. Such an ascending fluid would condense upon decompression to 150 bars pressure. (b) The line labeled V represents the isentropic ascent path of CO_2 from a hypothetical carbonatite reservoir. No phase changes are encountered before decompression to 1 bar pressure. (c) The I-V paths represent possible ascent paths of SO_2 from Ionian and/or terrestrial reservoirs (initial conditions given in detail by Kieffer, 1982a). Note that all paths, except V, enter multiple phase fields. (d) I-V paths represent possible paths of ascent of sulfur on Io, as discussed by Kieffer (1982b). Irreversible processes would swing the paths counterclockwise.

phase is not isentropic, as will be discussed below, the *T-S* diagrams provide a convenient reference for determination of paths of ascent and stable phases during different parts of the flow.

Consider first the ascent of the pure fluids illustrated. On the phase diagrams of Figure 11.4, possible initial conditions in different types of terrestrial and Ionian reservoirs are illustrated on the basis of estimated geotherms in different tectonic settings on the two planets (Figure 11.3). All plausible initial conditions give reservoir fluids that are highly compressed, liquid, or supercritical. As the fluids ascend from the supply regions or reservoirs in which they are initially at rest, their velocities are low because the volume changes associated with decompression are small as long as the fluids are in this compressed state. As they enter higher levels in the volcanic systems the fluids begin to expand, but two thermodynamically different processes may occur that would complicate the expansion (compare the left and right sides of the phase diagrams in Figure 11.4): (1) transformation (boiling) of a liquid (low-entropy) phase to a liquid-plus-vapor mixture and (2) transformation (condensation) of a vapor (high-entropy) phase to a vapor-plus-liquid mixture. Only the expansion of CO_2 from mantle conditions on the Earth (Figure 11.4b), or of SO_2 or S from a very high temperature reservoir on Io (Figures 11.4c and d), to ambient atmospheric pressure could occur without complications in the fluid flow due to phase changes. The effects of phase changes on erupting fluids have been qualitatively discussed by Kieffer (1982b).

The thermodynamic history and fluid-mechanical properties of a volatile phase are altered by the presence of entrained pyroclastic fragments. The entrained fragments increase the bulk density and effective molecular weight of the erupting fluid. They can also alter the expansion of the volatile phase by transferring heat to that phase. Two limiting cases are commonly considered: (1) if the entrained fragments are small, heat can be transferred from the solid fragments into the gas, and the gas will expand nearly isothermally, and (2) if the entrained fragments are large, heat cannot be effectively transferred to the gas and the gas will expand nearly adiabatically. If the process is reversible, the expansion is also isentropic. For many volcanic flows the ascent time is 10 to 100 sec, and particles less than a few millimeters in radius can be considered small in the sense of heat-transfer properties.

These considerations can be quantified in a simple way by assuming that the vapor-pyroclastic fragment mixture can be modeled as a pseudogas. The thermodynamic history of the solid and gas phases can be calculated separately (details are given in Appendix A of Kieffer, 1982b). A typical result for H_2O is shown in Figure 11.5, where the ascent path of H_2O alone from a hypothetical kimberlite reservoir is compared with the path of the H_2O if it contains a weight ratio m of pyroclastic fragments while it ascends. In many magmas, m lies in the range of 25 to 100. By these standards a relatively small weight fraction of entrained pyroclastic fragments ($m \geq 10$) can transfer sufficient heat to the vapor phase such that phase transformations do not occur until the fluid has decompressed to 1-bar pressure, when processes other than isentropic ascent influence the cooling history. However, the complications that

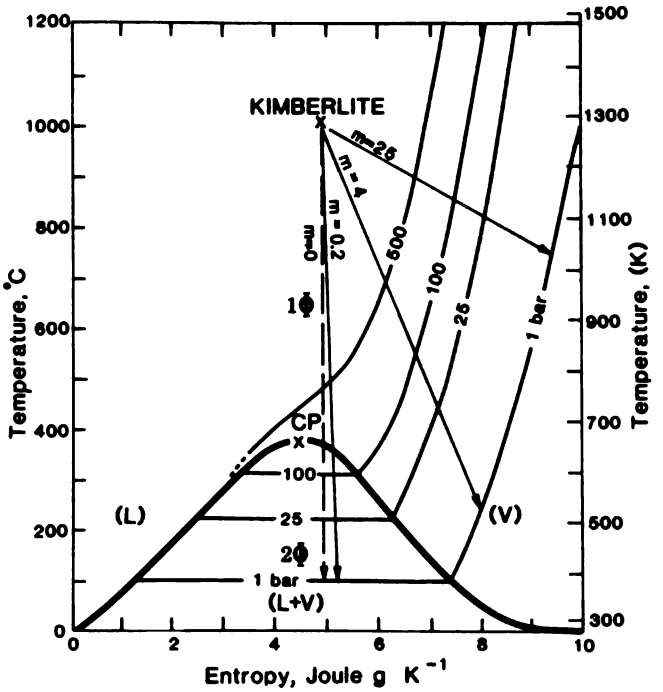

FIGURE 11.5 Temperature-entropy phase diagram for H_2O comparing the thermodynamic history of the H_2O during isentropic ascent of the fluid alone (m = 0 path) with isentropic ascent of a mixture containing weight ratio, m, of solids to vapor.

phase changes introduce into the fluid flow are avoided only at the expense of the complexities introduced into the flow by other processes, such as particle drag and heat transfer. I focus here on flows that contain sufficient entrained material such that phase changes do not complicate the flow.

The gross effects of pyroclastic mass and solid-gas heat transfer can be accounted for by the simple pseudogas model mentioned above, although particle drag is not considered. To obtain an equation of state for the erupting fluid suitable for use in the fluid flow equations, the erupting fluid is assumed to be a mixture of vapor and pyroclastic fragments through its entire ascent. Thus, in the following sections, reference to the properties of a "reservoir fluid" is to the properties of this vapor-particulate mixture in a hypothetical rest state not to the properties of the magma that physically exists there. The equation of state of a pseudogas-gas has the algebraic form of the perfect gas law:

$$PV = R_m T \tag{11.1a}$$

and

$$PV^{\gamma_m} = \text{constant}. \tag{11.1b}$$

In these equations, P is pressure, V is the volume of the mixture, T is absolute temperature, R_m is the gas constant, and γ_m is the isentropic exponent. Two modifications reflecting the *mixture*, rather than *vapor*, properties are that (1) the gas constant R_m is modified from the value appropriate to the vapor

alone, so that the mixture is modeled as a gas of high molecular weight, and (2) the value of γ_m is modified to account for heat-transfer processes within the expanding mixture. In the case of the flow duration being short and/or the entrained solids being so large that their heat cannot be appreciably transferred from the solids to the vapor, the isentropic exponent is left as that of the vapor phase alone, and the mixture expands adiabatically with the isentropic exponent of the vapor phase. In this case, γ_m is typically about 1.3. In the second case of the flow duration being long and/or the entrained solids being small (which allows appreciable heat transfer to occur rapidly), the isentropic exponent of the gas is modified to account for this heat flow. The *mixture* again expands adiabatically and isentropically, but the isentropic exponent for the mixture is close to unity, indicating that the *vapor* expansion is nearly isothermal. In most cases the latter assumption of flow with heat transfer is the most relevant one, and the flow expands with a very small value of γ_m. The specific volume, V, and the modified γ_m and R_m depend on the mass ratio, m, of solids to vapor (see equations in Kieffer, 1982b).

INITIAL THERMODYNAMIC CONDITIONS ASSUMED FOR THE RESERVOIRS

Initial conditions for the flow are determined in the supply and/or reservoir regions. It is here that differences in average temperature, pressure, and fluid composition (manifested in the weight ratio, m, and the gas constant, R, of the pseudogas equations) arise. Most current thermodynamic models for eruptions are similar to the one described above. In these models the thermodynamic behavior is independent of assumptions about the origin of the volatile phase (magmatic versus meteoric), except as the origin is reflected in the chosen values of P, T and m; as a result, the fluid-dynamic conclusions also are independent of these assumptions and cannot be used to test the classic problem of magmatic, phreatic, or phreatomagmatic origin of an eruption.

The differences in initial temperatures and compositions, however, are of secondary importance to the geometric factors in this discussion. The most important reservoir variable influencing overall jet structure is the ratio of initial reservoir pressure to atmospheric pressure. On Earth or on Io the range of tens of bars to perhaps a thousand bars brackets most initial reservoir pressures; for rare kimberlite eruptions on Earth, initial reservoir pressures may even be on the order of tens of thousands of bars. On Earth atmospheric pressure is approximately 1 bar; on Io ambient subsolar atmospheric pressure is between 10^{-12} and 10^{-7} bars; the pressure on the dark side could be as low as 10^{-17} bars. Hence, for different combinations of reservoir and atmospheric conditions, the ratio of reservoir to atmospheric pressure on Earth may be between ~10 and 10^5, and on Io between 10^{20} and 10^8.

The following reservoir conditions appropriate to the reservoirs shown in Figure 11.2 are assumed in order to focus the discussion, but the results are virtually insensitive to the values assumed:

1. For the Mount St. Helens lateral blast the reservoir fluid is assumed to have been a mixture of rock and H_2O vapor, with a mass ratio of solids to vapor of 25:1 (see Kieffer, 1982a, for details). On the basis of an average depth at which the blast material emanated from the mountain, the average initial pressure is assumed to have been 125 bars (appropriate to 650 m of lithostatic overburden) and the initial temperature to have been 600 K. This is the saturation temperature of pure H_2O at 125 bars and is perhaps a reasonable number to pick *a priori* in the absence of any information about the nature of the reservoir. This temperature may also be thought of as an averaged temperature of an erupting fluid that, after only a short distance of travel, was a thoroughly mixed fluid of hot dacite, hydrothermally altered rock and water, and glacial ice and organic debris. It therefore does not imply that the original reservoir nor the eruption that followed was strictly "hydrothermal." The median grain size in the blast material was less than 1 mm (Moore and Sisson, 1982), so there was good heat transfer between the particles and the vapor. Assuming continuous thermal equilibration of the particles and vapor, the value of γ_m for this mixture is 1.04.

2. For the Mount St. Helens plinian eruption, an initial pressure of 1000 bars (appropriate to a reservoir with an average depth of 3 km) and an initial temperature of 1200 K (approximately the liquidus temperature for the Mount St. Helens dacite) were assumed. The same mass ratio of solids to vapor of 25:1 as for the lateral blast was assumed for simplicity, so that the effective value of γ_m is 1.04. Variations of the value of γ_m to more nearly match the water content of the dacite would not significantly alter γ_m.

3. For Ionian volcanoes a variety of reservoir conditions and reservoir fluids, SO_2 and S with and without entrained pyroclastic fragments, were examined (details are given in Kieffer, 1982b). For discussion here I will assume an initial reservoir pressure of 40 bars and an initial temperature of 1000 K—higher than has yet been observed on Io but chosen specifically to provide an upper limit comparable to the Mount St. Helens case. A value of $\gamma_m = 1.1$ can be used to model either pure S_6 vapor or SO_2 vapor with a pyroclastic mass loading ratio of solids to vapor of $m = 1{:}1$.

FLUID-DYNAMIC CONDITIONS

Equations

The supply and reservoir regions have been defined above as places where the fluid is at, or nearly at, rest and the conduit as the place within the volcanic system where the fluid obtains an appreciable velocity. Therefore, the first stage in calculation of fluid motion is calculation of flow conditions in the conduit.

Flow is governed by the laws of conservation of mass, momentum, energy, and entropy. For simplicity, quasi-one-dimensional steady flow is examined. The general equations of motion are as follows:

$$\frac{1}{\rho}\frac{d\rho}{dz} + \frac{1}{u}\frac{du}{dz} + \frac{1}{A}\frac{dA}{dz} = 0 \qquad \text{(continuity) (11.2)}$$

$$\rho u \frac{du}{dz} + \frac{dP}{dz} \pm G + \frac{2}{D} f \rho u^2 = 0 \quad \text{(momentum) (11.3)}$$

$$\frac{d}{dz}\left(h + \frac{u^2}{2} + \psi\right) = 0 \quad \text{(energy) (11.4)}$$

$$dS \geq dQ/T. \quad \text{(entropy) (11.5)}$$

In these equations, z is the vertical coordinate, ρ is density, u is velocity, A is cross-sectional area, G is a body force (gravity), h is enthalpy, ψ is a field potential ($\psi_{,k} = -G_k$), D is the conduit diameter, and f is the Fanning friction factor ($f = 2\tau/\rho u^2$, where τ is the shear stress at the boundary of the fluid). S is entropy and Q is heat added to the system. The flow is assumed to be adiabatic and isentropic. Because field observations suggest that conduits are approximately straight, flow in the conduit is assumed to be strictly one-dimensional ($dA/dz = 0$); all significant area changes are assumed to occur in the crater. For this discussion the roles of gravity and friction during flow in the conduit and crater are ignored.

The integrated form of the conservation of energy Eq. (11.4) gives the well-known Bernoulli equation, which holds for thermodynamic states along any streamline:

$$h_0 + u^2/2 + \psi_0 = h_1 + u^2/2 + \psi_1, \quad (11.6)$$

where the subscripts 0 and 1 refer, respectively, to reservoir and flow conditions. For purposes of simple illustration, choose $u_0 = 0$ and ignore the gravity terms. Then

$$h_0 = h_1 + u^2/2. \quad (11.7)$$

This equation shows that the velocities obtained by fluids in explosive volcanism result from the simple conversion of the initial enthalpy of the fluid into kinetic energy (enthalpy = internal energy + energy stored in P-V compression, where P is pressure and V is volume). Latent heat of phase changes, exsolution of gases, or chemical reactions would be energetically similar to combustion terms in the above equations and must, of course, be included in a generalized form of this equation, but as will be shown below, their heat is not required to obtain large velocities of eruption and their effect is generally believed to be small during actual eruptions.

Flow in Conduits

The acceleration of the fluid as it moves from the reservoir through the volcanic system depends primarily on the pressure difference between the reservoir and the atmosphere into which the volcano is erupting and, secondly, on frictional and gravitational forces and on details of fluid properties. For the examples of interest on Earth and Io, atmospheric pressure is sufficiently less than the reservoir pressure, so that very large accelerations from initial to final pressure are possible. However, *accelerations within the conduit are limited by the geometry*. This limitation is best described with reference to the local fluid sound speed, a thermodynamic property that depends primarily on the fluid composition and temperature. For the pseudogas model used here, the reservoir sound speed is

$$c_0 = (\gamma_m R_m T)^{1/2}. \quad (11.8)$$

For the Mount St. Helens lateral blast fluid, c_0 was 105 m/sec; for the plinian fluid it was 150 m/sec; and for the Ionian reservoir fluid, it is about 220 m/sec. As the fluid accelerates up the conduit the flow velocity increases, but the sound velocity decreases because the temperature drops as the fluid expands. The fluid can accelerate within the conduit *only until the local flow velocity, u, equals the local sound velocity, $c^* = [2/(\gamma_m + 1)]^{1/2} c_0$.*

The conservation equations show that the fluid cannot accelerate above this velocity unless the conduit diverges. In my conceptualized volcanic system all significant divergences occur in the near-surface region defined as the surface crater. Thus, in a narrow, nearly straight conduit the flow velocity is approximately limited to the sonic velocity, a condition known as *choked flow*. Pressure, temperature, and density decrease until they reach the sonic conditions; to an order of magnitude, frictional effects do not change the results of this discussion. Typically, for vapor-particulate mixtures, sonic flow velocities are 100 to a few hundred m/sec, depending on the temperature and the solid-loading factor, m. For the examples here the sonic flow velocities are very close to the original reservoir sound speeds: Mount St. Helens blast, 104 m/sec; Mount St. Helens plinian column, 148 m/sec; and Ionian jets, 213 m/sec.

The pressure obtained at sonic conditions is

$$P^* = P_0 \left[\frac{2}{\gamma_m + 1}\right]^{\gamma_m/(\gamma_m - 1)} \quad (11.9)$$

For the Mount St. Helens lateral blast model, $P_0 = 125$ bars and $P^* = 75$ bars. The fluid volume increases by a factor of 1.64 from reservoir to sonic conditions. At sonic conditions, $T^*/T_0 = 2/(\gamma_m + 1) = 0.98$ for the proposed mixture. These pressure, volume, and temperature changes show that the initial sonic velocity of 104 m/sec is obtained by decompression of the reservoir fluid to 0.60 of the initial pressure, with accompanying volume expansion of a factor of 1.64 and conversion of only 2 percent of the internal energy into kinetic energy.

Sonic pressures are typically about half of the initial pressure for the fluids considered here, i.e., they are typically a few tens to a few hundreds of bars. These pressures are higher than the atmospheric pressure on Earth by factors of tens to hundreds and are higher than atmospheric pressure on Io by at least 8, and possibly 14, orders of magnitude! Thus, if the fluid emerged directly from the conduit into the atmosphere, it would be at a higher pressure than atmospheric, a condition discussed further below.

The high fluid pressures that exist in fluid erupting directly from a straight conduit or fracture cause surface craters to form, either by direct erosion of the sharp lips of such features or indirectly by slumping of unstable near-surface material into the flow (which has a great capacity for material transport in this relatively high pressure state; see discussion in Kieffer, 1982b). Surface craters are ubiquitous over most volcanic conduits associated with high-velocity jets on Earth. What effect do they have on the properties of the erupting fluid and, in particular, on pressure?

Flow in Craters

The area across which the fluid flows increases rapidly if it flows through a surface crater. For example, in Figure 11.6 a crater with internal slopes at angle of repose (30°) is shown overlying a conduit with a 5-m radius. As shown by the four columns on the right, the ratio of crater area to conduit area, A/A^*, increases dramatically with height above the crater floor. At a height of 200 m above the conduit, the crater has 5000 times the area of the conduit. This increasing area affects all of the flow variables. Application of Eqs. (11.1-11.5) allows all flow variables to be calculated within the framework of the quasi-one-dimensional approximation. The flow picks up speed, accelerating from Mach 1 at sonic conditions in the conduit to very high Mach numbers in the crater, and the temperature and density of the fluid decrease. Most importantly, for the discussion here, the pressure decreases substantially (Figure 11.6). There is about an order of magnitude difference in the rate of pressure decrease depending on the properties of the vapor phase and/or the amount of heat transfer, as manifested in different values of γ_m (values for γ_m of 1.3 and 1.04 are shown in Figure 11.6). However, compared with a pressure drop of only about 50 percent obtained during flow between the reservoir and the top of the conduit, the decrease in pressure by many orders of magnitude within even short distances in the crater is dramatic, e.g., it decreases nearly five orders of magnitude in the first 200 m.

Within a crater, then, the fluid pressure will tend to drop toward ambient atmospheric pressure simply because of the area change. On Earth, a pressure drop by a factor of 100 to 1000 would be sufficient to reduce the fluid pressure to ambient atmospheric pressure. This can happen within a shallow surface crater—one with a depth of tens of meters. (In fact, the effect of friction alone in a very long conduit could reduce the fluid pressure to ambient on Earth without a surface crater if initial reservoir pressures were on the low side of normal reservoir values.) Thus, *in most cases of terrestrial volcanism where there are even minor surface craters, jets enter the atmosphere with a fluid pressure approximately equal to ambient atmospheric pressure*, a condition that I will call *pressure balanced*. If they enter the atmosphere at a pressure significantly above ambient, I call them *overpressured*, although the commonly used description in fluid mechanics is *underexpanded*.

On Io, ambient atmospheric pressure is about 10^{-12} bars but could be higher (10^{-7} bars?) around volcanic eruption sites. With typical reservoir pressures on the order of tens of bars, a pressure drop of about 8 to 15 orders of magnitude is required to reduce the volcanic fluid pressure to ambient pressure. A crater on the order of 1000 m or deeper would be required for this depressurization. Thus, there is the possibility of pressure-balanced jets occurring on Io *if and only if* they erupt from volcanic systems with craters more than 1 km deep. The jets will be overpressured if the eruptions occur through shallow craters or fissures without craters.

These conclusions depend on the assumed conduit-crater geometry. The amount of depressurization is directly proportional to the ratio of crater to conduit area, as can be seen from Figure 11.6. The conduit dimension chosen, 5-m radius, is representative of terrestrial dikes that might be interpreted as conduits of ancient volcanoes. Therefore, the minimum crater depth of about 1 km referred to above as necessary for creation of a pressure-balanced jet on Io applies *if* the geometry of Ionian volcanic systems is similar to those postulated for Earth. However, if the conduit-crater geometry were drastically different,

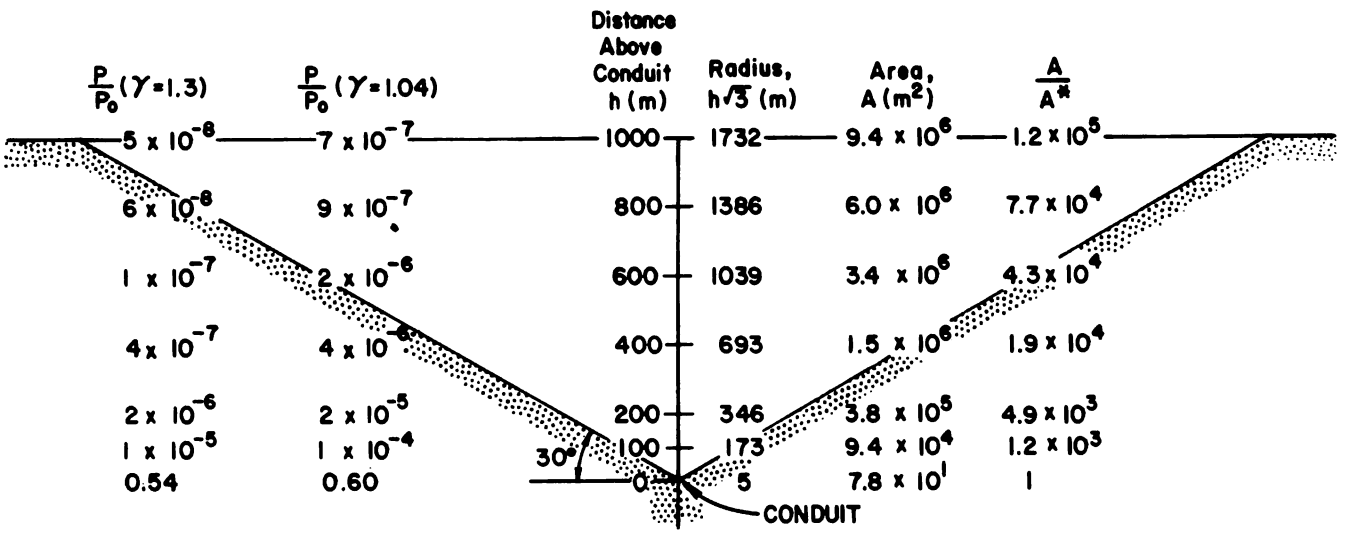

FIGURE 11.6 Variation of geometric and flow variables in crater. For this nominal geometry the conduit radius has been taken as 5 m, and the crater has been taken with the internal slopes at angle of repose, 30° from horizontal. The two central columns give height above the crater floor (in meters) and the ratio of crater area, A, to conduit area, A^*. The columns on the far right and far left give the ratio of fluid pressure, P, to reservoir pressure, P_0, for the two values of γ_m shown (from Kieffer, 1982b, modified and reproduced with permission of the University of Arizona Press).

e.g., if a conduit had a radius of 500 m and the surface crater were as postulated above, the inferred depth at which pressure equilibration would occur would need to be scaled to the place in the crater where comparable area ratios, A/A^*, were obtained. Similarly, if the crater were simply a gradual steep-walled enlargement of the conduit, as proposed by Hawthorne (1975) for kimberlite geometries, the pressure equalization distances would also need to be scaled. In Hawthorne's model of a kimberlite pipe, the conduit enlarges by a factor of 100 over the top 2.5 km of its profile. For a fluid with γ_m in the range of 1.0 to 1.1, the pressure at the exit plane would be 0.1 percent of the stagnation pressure (assumed to be the reservoir pressure in this model that ignores friction). If the initial reservoir pressure were 1 kbar, the jet could become pressure-balanced traversing 2.5 km through this steep-walled geometry. At higher pressures plausible for kimberlite reservoirs, passage through a conduit of such a geometry would not (in the absence of friction) reduce the jet pressure to ambient, and it would exit as an overpressured jet.

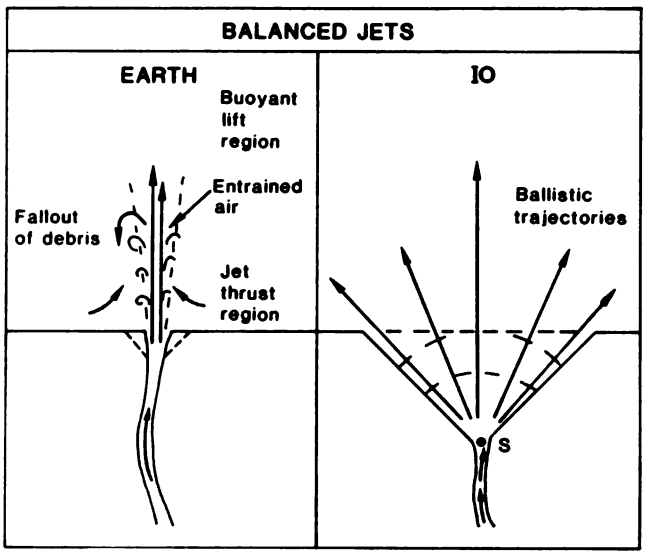

FIGURE 11.7 Schematic drawings of the structure of pressure-balanced jets on Earth and on Io.

IMPLICATIONS FOR JET STRUCTURE

Pressure-Balanced Jets

Pressure-balanced and overpressured jets have different structures because of the respective absence and presence of internal-pressure gradients. Their structures are summarized in Figures 11.7 and 11.8.

In a pressure-balanced jet under terrestrial conditions, the flow maintains a direction approximately parallel to the centerline of the conduit in which the fluid accelerates, because internal pressure gradients that could cause it to expand laterally are dissipated by passage through a small crater (Figure 11.7a). Thus, flow is unidirectional in terrestrial pressure-balanced jets, the initial velocity vector is parallel to the centerline of the volcanic conduit, and the jets have no internal wave structures because of pressure gradients. Plinian jets on Earth (Figure 11.1a) are usually pressure balanced because they rise through long conduits (in which friction helps reduce the pressure toward ambient) and/or shallow surface craters. In the case of the plinian column on May 18 at Mount St. Helens, the jet probably rose through a conduit on the order of 3 km long and through a small crater in the floor of the amphitheater created by the lateral blast (inferred from the morphology of the crater floor after cessation of the eruption). If this crater had been only a few tens of meters deep, it would have been sufficiently deep to allow decompression to 1-bar pressure. Such plinian jets rise upward in the atmosphere *not* because of internal pressure of the gas but through a combination of initial momentum combined with increasing buoyancy as air is entrained into the jet (these are the jets carefully studied and modeled by Wilson, 1976; Sparks *et al.*, 1978; Wilson *et al.*, 1980; see also Wilson and Head, 1983).

The structure of pressure-balanced jets on Io might be expected to be quite different from those on Earth, not only because of the effects of different gravity and atmospheric pressure but also because of the much deeper crater required to produce a pressure-balanced jet on Io (Figure 11.7). The high internal pressure (relative to the ambient pressure) that causes the flow to expand laterally will be maintained through a fairly large crater traverse, and the flow streamlines will diverge to become parallel to the crater walls. As the flow traverses the surface crater, fluid pressures drop from several bars to atmospheric pressure. The velocity vectors tend to depart more from the initial vertical direction imparted by accelerations in the restricted conduit. Within the crater, flow streamlines will not be parallel to the centerline of the conduit nor perpendicular to planes across the crater; rather they diverge as the flow follows the contours of the crater. A rigorous model of the flow would require two- or three-dimensional flow equations in the crater. However, to a first approximation the spreading streamlines diverge from an apparent spherical center of symmetry at the bottom of the crater. Surfaces of constant flow properties are, then, hemispheres rather than planes. Strom and Schneider (1982) showed that the shape and optical characteristics of the umbrella jet at plume 3, Prometheus, can be well modeled by using a point-source ballistic model in which particles radiate with a uniform velocity through angles from 0 (vertical) to 55 (about angle of repose). I suggest that this is because Prometheus (Figure 11.1c) and, by analogy, the umbrella jets are pressure-balanced jets, in which internal-pressure gradients are negligible. After passage through the surface crater, the gas and the particles coupled to the gas follow simple ballistic trajectories in the near-vacuum environment of the Ionian surface. These ballistic trajectories are determined as the streamlines of the flow diverge to follow the crater walls. From this analysis it can be inferred that the jet of Prometheus emerges from a rather deep surface crater ($> \sim 1$ km). [Note that the surface crater discussed here is several kilometers in diameter (see Figure 11.6), which is below the limits of resolution of Voyager images.]

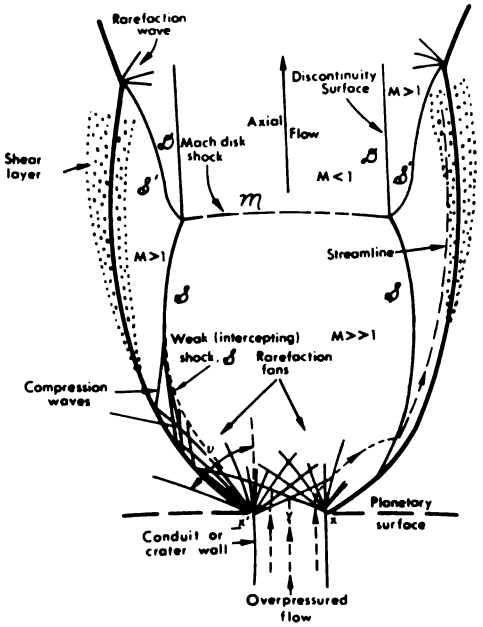

(a)

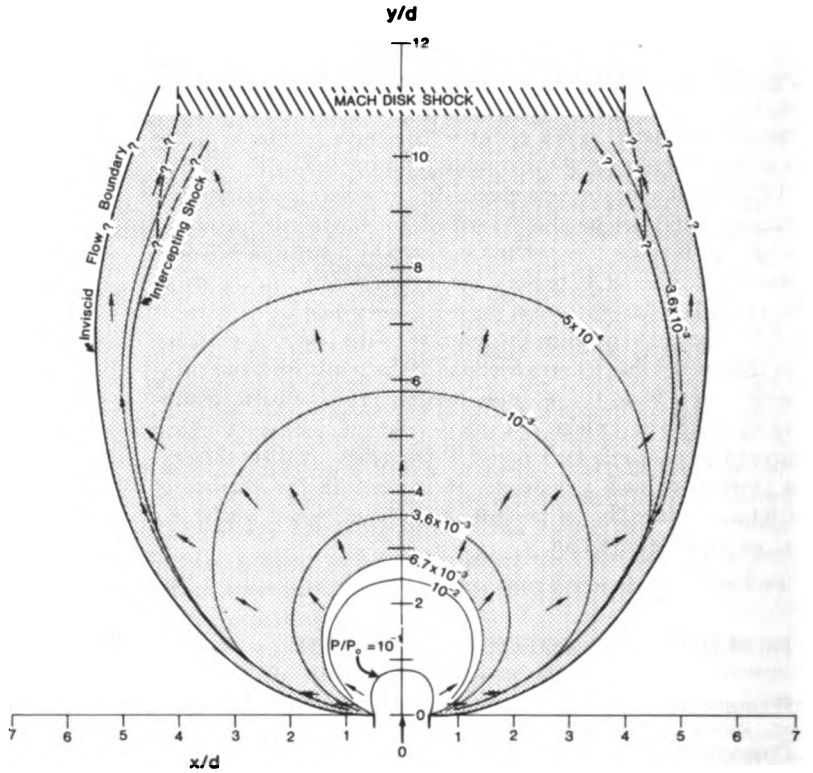

(b)

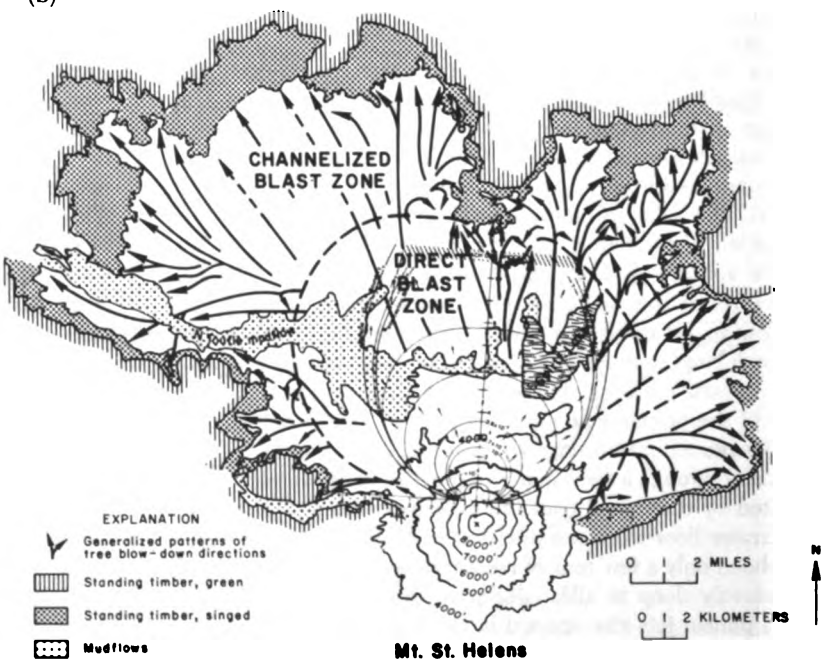

(c)

FIGURE 11.8 (a) Schematic drawing of an overpressured jet (from JANNAF, 1975). (b) Conditions in the supersonic part of the flow during the lateral blast on May 18, 1980, at Mount St. Helens. Calculations from the Lockheed Plume Code (courtesy of R. A. O'Leary, Rocketdyne, division of Rockwell International). All length dimensions, x and y, are normalized to vent diameter, d. The boundary of the flow is assumed to have been at constant pressure 8.7×10^4 Pa (0.87 bar); the reservoir is assumed to have initially been at 12.5 MPa (125 bars). The flow is assumed to have been choked at Mach 1 at the vent; the exit Mach number of the flow is taken as 1.02 to ease numerical computation problems. Contours of constant thermodynamic properties are shown, as summarized in Table 11.1. Small arrows indicate the local flow direction. The flow diverges through rarefaction waves (not shown; see Figure 11.8a for schematic representation) that reflect from the flow boundaries to form the intercepting shocks shown. Across these shocks the flow velocities decrease, the pressure increases, and the flow changes direction. The intercepting shocks coalesce across the flow to form the strong Mach disk shock. In most of the flow the pressure is subatmospheric (stippled zone). It rises back toward atmospheric across the Mach disk and intercepting shocks. The location of the Mach disk shock is not predicted by the computer code; it is estimated from the JANNAF (1975) equations. (c) Figure 11.8b, scaled to and superposed on the devastated area at Mount St. Helens (same orientation and placement as in Kieffer, 1982a). Note approximate coincidence of supersonic jet and direct blast zone.

TABLE 11.1 Thermodynamic Conditions on the Contours in Figure 11.8B

P/P_0	M	T/T_0	ρ/ρ_0
1.0×10^{-1}	2.1	0.92	1.9×10^{-1}
1.0×10^{-2}	3.1	0.84	1.8×10^{-1}
6.7×10^{-3} (ambient)	3.3	0.82	1.4×10^{-2}
3.6×10^{-3}	3.5	0.80	6.9×10^{-3}
1.0×10^{-3}	3.9	0.76	2.0×10^{-3}
5.0×10^{-4}	4.1	0.75	1.1×10^{-3}

Overpressured Jets

The structure of overpressured jets, shown in Figure 11.8a, is much more complex than that of pressure-balanced jets because there are initially large pressure gradients within the jet. These pressure gradients cause the jet to expand through rarefaction or expansion waves that emanate from the sides of the vent. The fluid thus diverges from its initial centerline direction (flares strongly) near the vent, and streamlines of the flow diverge from the simple paths determined in the conduit. If the fluid is at substantially higher pressure than ambient, it does not simply expand to ambient pressure as it emerges but actually overexpands, developing a low-pressure zone in the center of the flow. The atmosphere then presses back in on the fluid, causing the flow boundaries to curve around to become more subparallel to the initial direction of flow. A complex system of internal expansion, compression, and shock waves is set up in response to the decompression. These internal waves, as well as gravity, turbulence, air entrainment, buoyancy, and atmospheric structure, must be considered in models of jet structure.

Equations of motion for an axisymmetric jet, in the absence of viscous forces and of gravitational accelerations, are as follows:

$$\bar{\nabla} \cdot (\rho \bar{u}) = 0 \qquad \text{(continuity) (11.10)}$$

$$\bar{\nabla} \times \bar{u} = 0 \qquad \text{(irrotationality) (11.11)}$$

$$\bar{\nabla}\left(\frac{u^2}{2}\right) + \frac{1}{\rho}\bar{\nabla} P = 0. \qquad \text{(momentum) (11.12)}$$

In these equations, ρ is the density, $\bar{u}$ is the vector velocity, P is the pressure, and $\bar{\nabla}$ is the spatial differential operator. The equations are nonlinear and not solvable analytically. Detailed structure of overpressured jets is difficult to calculate because internal shock waves are difficult to handle mathematically, even with the aid of large computers. Within regions of flow where there are no strong shock waves, solutions can be obtained by the method of characteristics. A solution for the initial conditions proposed for the Mount St. Helens lateral blast obtained by hand calculations was given by Kieffer (1982a); a refined computer-generated version is given here in Figure 11.8b. In such solutions the position of strong shocks must be determined independently, e.g., from compilations of laboratory data, such as JANNAF (1975) or Ashkenas and Sherman (1966). The major features of the two models are in good agreement. However, a significant difference is the curvature of the boundary of the supersonic region. In the model given by Kieffer (1982a) the boundary was determined by use of the JANNAF (1975) construction formula; its use for the pressure ratios assumed for the blast represented an extrapolation beyond limits validated by laboratory experiment. As a result, the new theoretical boundary is preferable even though the discrepancy with the mapped boundary between the direct and channelized blast zones is increased.

Because the computer-generated flow field presented is so similar to the model given by Kieffer (1982a), detailed discussion of the flow-field properties will not be repeated here. However, several points are worth reemphasizing because of their relevance to jet structure, and several new quantitative statements can be made.

First, the flow originally emanating northward from the vent is immediately deflected through a range of angles, up to 96°. Thus, highly overpressured jets do not form simple fire-hydrant-shaped jets; instead they form fan-shaped ones. The flow is turned back more nearly parallel to the initial flow direction as it passes through the intercepting shocks (see Figure 11.8b, small arrows).

Second, much of the region within the flow is at subatmospheric pressure (the stippled region in Figure 11.8b). The atmosphere responds to the formation of this low-pressure zone by pressing inward, causing the intercepting and Mach disk shocks to form. The pressure drops to 4 percent of atmospheric pressure immediately in front of the Mach disk shock. When the fluid passes through the lateral intercepting shocks and the Mach disk shock, the pressure is brought back up toward atmospheric.

Third, everywhere in the flow, except possibly for a small region right in front of the Mach disk shock, the density of the fluid remains greater than the atmospheric density. (Uncertainties in the computer handling of the convergence of the lateral intercepting shocks preclude a statement on whether there is actually a small region that decompresses to or below atmospheric density.) Thus, with the possible exception of a small "chimney" in front of the Mach disk shock, the flow is negatively buoyant within the supersonic zone. At the inviscid boundary of the supersonic plume, the density is 0.014 g/cm^3, about 16 times atmospheric density. In front of the Mach disk shock it is approximately atmospheric density or slightly less; upon passing through the Mach disk shock the density also increases. In my original work (1982a) I assumed that the Mach disk shock was a weak shock; thus, I extrapolated the densities through the shock. An alternative and better-founded assumption (Ashkenas and Sherman, 1966) is that the Mach disk shock is a strong shock that brings the flow pressure back to atmospheric; in this case the density of the fluid increases to about 10 times atmospheric. Thus, at the margins of the supersonic flow region, the fluid is denser everywhere than in the atmosphere. The temperature of the fluid also increases dramatically as it passes through the Mach disk shock. Thus, the shock could be a source of both major flow disturbances and atmospheric phenomena because of the pressure, density, and temperature changes (see Chapter 10 of this volume).

Fourth, the "boundary" of the plume shown in Figure 11.8b is a boundary calculated by assuming inviscid flow. No esti-

mates of the conditions in the shear layer that exists on the flow boundary (shown in Figure 11.8a) are included, which means that the calculated flow velocities at the boundary are not realistic. The calculated inviscid flow velocities are about 300 m/sec. Entrainment and mixing would substantially reduce these velocities and would alter the density of the flow. The model strongly suggests, however, that around the perimeter of the supersonic zone the flow transforms from a supersonic jet to a dense, largely subsonic flow. Gravity would play a major role in the flow motion beyond the supersonic flow boundary.

When scaled to and superposed on a map of the devastated area at Mount St. Helens (Figure 11.8c), the overpressured jet mimics the shape of the direct blast zone, leading me to conclude that the direct blast zone was a zone dominanted by supersonic fluid flow and that the surrounding channelized blast zone was the zone of denser subsonic flow (Kieffer, 1982a). The model explains a number of features related to flow properties, such as velocity, density, downed-tree pattern, and temperatures throughout the devastated area. For example, internal rarefaction waves at the vent deflected the flow through more than a 90° angle initially, causing initial flow directions of some of the fluid to be approximately east-west. However, because the rarefaction waves were reflected from the boundary between the flow and the atmosphere as compressive waves, coalescing to form the Mach disk shock, the flow turned back to a more northerly direction as it diverged from the vent. Streamlines of overpressured flows are extremely complex, and all of the internal waves affect the velocities and direction of flow that crosses them. In fact, if streamlines from the lateral parts of the flow field near the source are extrapolated in a simple linear manner back toward the vent, they do not converge at the vent but rather at an apparent source at least 1 km in front of the actual vent. No actual physical source in such a location is required to explain the nature of such streamlines.

What would be the characteristics of an overpressured jet on Io? Internal-wave dynamics within the jet would destroy the smooth ballistic trajectories that give the umbrella shape to pressure-balanced jets on Io. Perhaps in low-resolution photos such jets would appear to be rather structureless blobs like the jet from Loki (Figure 11.1d) or, on a smaller scale, their deposits would be irregular like the white frost deposits described by McCauley et al. (1979). If diffuse jets do exist on Io and are indeed overpressured, it can be inferred that the internal fluid pressure at the vent is greater than atmospheric and that the jets originate from conduits or fissures that have only shallow surface craters.

It is at least consistent with the idea that the regolith of Io consists of interbedded pyroclastic material, sulfur lava flows, and perhaps some silicate ash, i.e., weakly cohesive material in which kilometer-deep volcanic craters could easily be excavated, that most of the plumes on Io are umbrella shaped. The two plumes that have at least at times been diffuse are Loki (plume 2) and Amirani (plume 5). These plumes emanate from fissures that are perhaps in sufficiently strong surface materials that deep craters are not easily eroded, so that overpressured plumes can at least be maintained temporarily. An intriguing implication of this model is that plume structure on Io could change substantially as atmospheric pressure changes, e.g., from day to night.

SUMMARY

The structure of pressure-balanced jets may vary from one planet to another, but on one planet the jets may tend to have rather similar structures from one volcano to another because they are equilibrated to atmospheric pressure. This is perhaps the reason that plinian jets around Earth look rather similar. However, overpressured jets may show a much greater diversity in structure because pressure imbalances may range from slight ($P > P_a$) to huge ($P >>> P_a$), and jet structure depends on the degree of overpressurization. Thus, either as a class, or as individuals like the Mount St. Helens blast, overpressured jets are harder to categorize, analyze, and model. This paper describes the role of compressibility, without considering the influences of other important effects, such as gravity; buoyancy; viscous effects at boundary layers; and, for lateral jets, topography. Accurate prediction of hazards from jets during explosive eruptions must account simultaneously for the influence of all of these effects.

REFERENCES

Ashkenas, H., and F. S. Sherman (1966). The structure and utilization of supersonic free jets in low density wind tunnels, in *Rarified Gas Dynamics*, Vol. 2, Academic Press, New York, pp. 84-105.

Boyd, F. R. (1961). Welded tuffs and flows in the rhyolite plateau of Yellowstone National Park, Wyoming, *Geol. Soc. Am. Bull. 72*, 387-426.

Graton, L. C. (1945). Conjectures regarding volcanic heat, *Am. J. Sci. 243A*, 135-259.

Hawthorne, J. B. (1975). Model of a kimberlite pipe, *Phys. Chem. Earth 9*, 1-16.

JANNAF [Joint Army, Navy, NASA, Air Force] (1975). *Handbook of Rocket Exhaust Plume Technology*.

Kieffer, S. W. (1981). Blast dynamics at Mount St. Helens on 18 May 1980, *Nature 291*, 568-570.

Kieffer, S. W. (1982a). Fluid dynamics of the May 18 blast at Mount St. Helens, in *The 1980 Eruptions of Mount St. Helens, Washington*, P. W. Lipman and D. R. Mullineaux, eds., U.S. Geol. Surv. Prof. Pap. 1250, pp. 379-400.

Kieffer, S. W. (1982b). Ionian volcanism, in *Satellites of Jupiter*, D. Morrison, ed., U. Arizona Press, Tucson, pp. 647-723.

McCauley, J. F., B. A. Smith, and L. A. Soderblom (1979). Erosional scarps on Io, *Nature 280*, 736-738.

McEwen, A. S., and L. A. Soderblom (1983). Two classes of volcanic plumes on Io, *Icarus 55*, 191-217.

Moore, J. A., and W. C. Albee (1982). Topographic and structural changes March-July 1980—photogrammetric data, in *The 1980 Eruptions of Mount St. Helens, Washington*, P. W. Lipman and D. R. Mullineaux, eds., U.S. Geol. Surv. Prof. Pap. 1250, pp. 123-134.

Moore, J. A., and T. W. Sisson (1982). Deposits of the May 18 pyroclastic surge, in *The 1980 Eruptions of Mount St. Helens, Washington*, P. W. Lipman and D. R. Mullineaux, eds., U.S. Geol. Surv. Prof. Pap. 1250, pp. 421-438.

Self, S., L. Wilson, and I. A. Nairn (1979). Vulcanian eruption mechanisms, *Nature 277*, 440-443.

Sparks, R. S. J. (1978). The dynamics of bubble formation and growth in magmas: A review and analysis, *J. Volcanol. Geotherm. Res. 3*, 1-37.

Sparks, R. S. J., L. Wilson, and G. Hulme (1978). Theoretical modeling of the generation, movement, and emplacement of pyroclastic flows by column collapse, *J. Geophys. Res. 83*, 1727-1739.

Strom, R. G., and N. M. Schneider (1982). Volcanic eruption plumes on Io, in *Satellites of Jupiter*, D. Morrison, ed., U. Arizona Press, Tucson, pp. 598-633.

Strom, R. G., R. J. Terrile, H. Masursky, and C. Hansen (1979). Volcanic eruption plumes on Io, *Nature 280*, 733.

Verhoogen, J. (1946). Volcanic heat, *Am. J. Sci. 244*, 745-770.

Wilson, L. (1976). Explosive volcanic eruptions—III. Plinian eruption columns, *Geophys. J. R. Astron. Soc. 45*, 543-556.

Wilson, L., and J. W. Head III (1983). A comparison of volcanic eruption processes on Earth, Moon, Mars, Io and Venus, *Nature 302*, 663-669.

Wilson, L., R. S. J. Sparks, and G. P. L. Walker (1980). Explosive volcanic eruptions—IV. The control of magma properties and conduit geometry on eruption column behavior. *Geophys. J. R. Astron. Soc. 63*, 117-148.